RESEARCH ARTICLE

Key Points:
- Long-term fertilization shifts N cycling in salt marsh sediments from retention to removal
- Denitrification was tightly coupled to nitrification in salt marsh sediments

Supporting Information:
- Supporting Information S1

Correspondence to:
X. Peng,
nickpeng@geol.ucsb.edu

Long-term fertilization alters the relative importance of nitrate reduction pathways in salt marsh sediments

Xuefeng Peng[1,2], Qixing Ji[2], John H. Angell[3], Patrick J. Kearns[3,4], Hannah J. Yang[2], Jennifer L. Bowen[3,4], and Bess B. Ward[2]

[1]Now at Department of Earth Science and Department of Chemical Engineering, University of California, Santa Barbara, California, USA, [2]Department of Geosciences, Princeton University, Princeton, New Jersey, USA, [3]Department of Biology, University of Massachusetts, Boston, Massachusetts, USA, [4]Now at Department of Marine and Environmental Science, Northeastern University, Nahant, Massachusetts, USA

Abstract Salt marshes provide numerous valuable ecological services. In particular, nitrogen (N) removal in salt marsh sediments alleviates N loading to the coastal ocean. N removal reduces the threat of eutrophication caused by increased N inputs from anthropogenic sources. It is unclear, however, whether chronic nutrient overenrichment alters the capacity of salt marshes to remove anthropogenic N. To assess the effect of nutrient enrichment on N cycling in salt marsh sediments, we examined important N cycle pathways in experimental fertilization plots in a New England salt marsh. We determined rates of nitrification, denitrification, and dissimilatory nitrate reduction to ammonium (DNRA) using sediment slurry incubations with ^{15}N labeled ammonium or nitrate tracers under oxic headspace (20% oxygen/80% helium). Nitrification and denitrification rates were more than tenfold higher in fertilized plots compared to control plots. By contrast, DNRA, which retains N in the system, was high in control plots but not detected in fertilized plots. The relative contribution of DNRA to total nitrate reduction largely depends on the carbon/nitrate ratio in the sediment. These results suggest that long-term fertilization shifts N cycling in salt marsh sediments from predominantly retention to removal.

1. Introduction

Salt marshes not only possess aesthetic beauty but also provide a number of valuable ecological services, such as storm protection [*Moller et al.*, 2014]; carbon storage [*Duarte et al.*, 2005]; and providing nursery grounds for numerous species of birds, fish, and invertebrates [*Teal and Howes*, 2000]. As the interface between terrestrial and marine ecosystems, salt marshes intercept and remove a significant amount of nutrients arriving from upstream, alleviating the nutrient loading into the coastal ocean [*Sousa et al.*, 2008]. Nitrogen (N) is one of the main nutrients that is processed and removed from salt marsh sediments.

One of the main N removal pathways in coastal marine sediments is denitrification, the largely anaerobic reduction of nitrate (NO_3^-) to dinitrogen gas (N_2). Salt marshes, characterized by extraordinarily high primary productivity, can remove large amounts of land-derived N and can reduce eutrophication via their high rates of sedimentary denitrification and plant uptake [*Sousa et al.*, 2008; *Drake et al.*, 2009]. In salt marsh sediments, denitrification is usually tightly coupled to nitrification, the aerobic oxidation of ammonium (NH_4^+) to nitrite (NO_2^-) and subsequently NO_3^- [e.g., *Hamersley and Howes*, 2005; *Patrick and Reddy*, 1976]. Transport of oxygen into anoxic depths of sediments via the aerenchyma of salt marsh plants facilitates the coupling between nitrification and denitrification [*Arenovski and Howes*, 1992].

Alternatively, NO_3^- in coastal marine sediments can be reduced to NO_2^- and then converted to N_2 by anaerobic ammonia oxidation (anammox). After being observed in natural environments over a decade ago [*Thamdrup and Dalsgaard*, 2002], anammox has been measured along with denitrification in a wide range of coastal marine sediments. The contribution of anammox to N loss is variable and not well constrained. In organic rich coastal sediments, the relative importance of anammox is thought to be low [*Engstrom et al.*, 2005], and one study showed that anammox accounted for < 3% of total N loss from salt marsh sediments [*Koop-Jakobsen and Giblin*, 2009].

Dissimilatory nitrate reduction to ammonium (DNRA) is another NO_3^- reduction pathway that is potentially important in coastal marine sediments, but early investigations often neglected DNRA [*Burgin and Hamilton*, 2007]. Unlike denitrification and anammox, DNRA does not produce N_2. Instead of removing fixed

nitrogen, DNRA contributes to the internal cycling of the fixed N pool. In coastal ecosystems, including salt marshes, the relative importance of DNRA in NO_3^- reduction is highly variable and the number of studies is limited [*Giblin et al.*, 2013; *Song et al.*, 2013]. Whole-core incubations showed a sixfold increase in DNRA rates after 5 years of NO_3^- fertilization in salt marsh sediments [*Koop-Jakobsen and Giblin*, 2010]. On the other hand, a clear negative correlation between DNRA rates and NO_3^- concentrations was observed in slurry incubations with salt marsh sediments from the coast of England [*King and Nedwell*, 1985].

Industrial production of fixed N via the Haber-Bosch process and agricultural application of fertilizers has tremendously accelerated N loading into salt marsh ecosystems. Widely distributed along the world's coastlines, salt marshes are directly affected by these anthropogenic sources of N [*Deegan et al.*, 2012]. Fertilization changes key factors that control the rate and relative contribution of each NO_3^- reduction pathway in salt marsh sediments, including organic carbon availability, NO_3^- availability, and the ratio of carbon to nitrogen (carbon/N) of the sediments [*Brin et al.*, 2015; *Dalsgaard et al.*, 2005; *Hardison et al.*, 2015; *Song et al.*, 2013]. How changes brought about by long-term fertilization ultimately affect the relative importance of denitrification and DNRA in salt marsh sediments was addressed in this study.

Previous studies directly measuring nitrate reduction rates in coastal marine sediments have commonly used the acetylene inhibition method [e.g., *Tiedje et al.*, 1982], ^{15}N-labeled substrates [e.g., *Nishio et al.*, 1983; *Risgaard-Petersen et al.*, 2003], and nitrogen-to-argon ratios [*Kana et al.*, 1998], which were applied to both whole-core and slurry incubations [*Groffman et al.*, 2006]. Whole-core incubations were generally performed with oxic overlying water [e.g., *Nishio et al.*, 1983; *Kana et al.*, 1998] or with oxic headspace [e.g., *Seitzinger et al.*, 1980]. Since the discovery of anammox in marine sediments, an updated isotope paring technique [*Risgaard-Petersen et al.*, 2003] applied to slurry incubations has been broadly adopted to measure rates of NO_3^-/NO_2^- reduction. While capable of distinguishing anammox from denitrification, this method employs anoxic headspace, which excludes aerobic nitrification as a source of nitrate and hence prevents coupled nitrification-denitrification [*Rysgaard et al.*, 1994]. Additionally, the concentrations of the [15]NO_3^- amendment (usually 50–200 μM) in previous studies often exceeded ambient levels [e.g., *Thamdrup and Dalsgaard*, 2002; *Risgaard-Petersen et al.*, 2004].

We used slurry incubations with ^{15}N-labeled tracers to measure nitrification, denitrification, and DNRA rates in the long-term fertilization plots at Great Sippewissett Marsh, Falmouth, MA, USA. The experimental plots at Great Sippewissett Marsh are rare in that they have been fertilized for over 40 years [*Valiela*, 2015; *Valiela et al.*, 1973], and hence, they are suitable for assessing the effects of long-term fertilization on N cycling in salt marsh sediments. This study was extensive in sampling scheme, covering both high- and low-marsh habitats in six experimental plots. Two specific aspects of our experimental design distinguished this study from previous studies using slurry incubations with ^{15}N-labeled substrates. First, all incubations were performed under oxic, instead of anoxic, headspace. This was a more realistic simulation of oxygen conditions in the field, and it allowed the occurrence of nitrification, which produced substrates for NO_3^- reduction. Second, the amount of ^{15}N-labeled substrates added was low relative to the ambient amount of substrates, in order to minimize perturbing the N cycling processes. Our results indicate that long-term fertilization shifts the relative proportions of denitrification and DNRA in salt marsh sediments.

2. Methods

2.1. Site Description and Sample Collection

The Great Sippewissett Marsh is located in West Falmouth Harbor on Cape Cod, Massachusetts, USA (41° 35′ 3.1″ N, 70° 38′ 17.0″ W). The long-term fertilization plots established since the early 1970s have been described previously [*Valiela*, 2015; *Valiela et al.*, 1973]. In brief, in addition to two unfertilized control plots (C), three dosages of mixed fertilizer (10% N, 6% P_2O_5, and 4% K_2O) [*Valiela et al.*, 1973] were applied biweekly during the growing season (late April through October) to duplicate plots (10 m in radius, Figure 1): 0.85 g N m^{-2} week^{-1} in low-fertilization plots (LF), 2.52 g N m^{-2} week^{-1} in high-fertilization plots (HF), and 7.56 g N m^{-2} week^{-1} in extra-high fertilization plots (XF). The slow-release fertilizer (Milorganite sewage pellets) is composed of 80% organic N, 16% NO_3^-, and 4% NH_4^+. In the rest of this paper, letter acronyms ("C," "LF," "HF," and "XF") are used to refer to the different experimental plots.
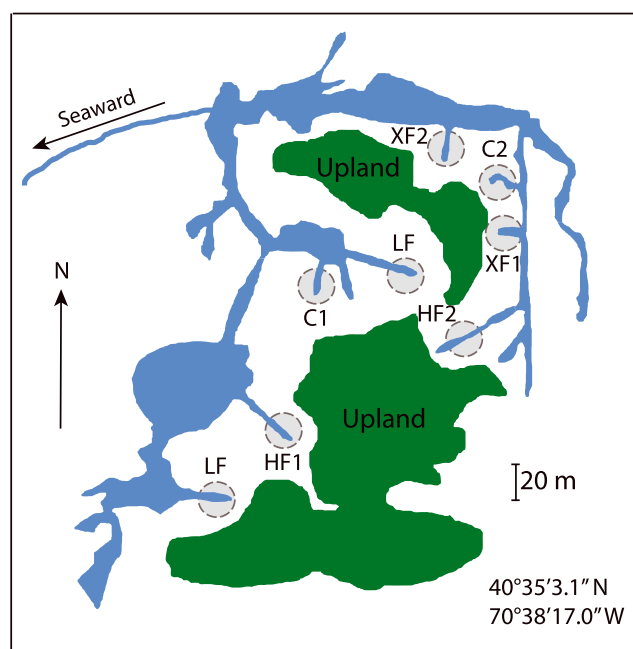
Figure 1. Map of experimental plots at the Great Sippewissett Marsh (adapted from *Fox et al*. [2012]). Letter acronyms C, LF, HF, and XF represent control, low fertilization, high fertilization, and extra-high fertilization, respectively.

A small creek bisects each plot. Marsh plants proximate to the creek bank (low marsh) are at a lower elevation compared to those farther away (high marsh). High-marsh habitats are about 135 cm above sea level on average, and low marshes are mostly 85 cm above sea level on average [*Fox et al*., 2012]. Local tides are diurnal, varying from 30 cm below sea level to 30 cm above sea level during low tides and from 110 to 180 cm above sea level during high tides (http://www.tides.info). Depending on the tidal level, high-marsh habitats were flooded twice a day for less than one to more than 4 h. Low-marsh habitats were flooded for at least 3 h during each high tide. In most plots, tall and short forms of *Spartina alterniflora* dominate the low and high marsh, respectively. The only exception is the high marsh in XF plots, where *Distichlis spicata* dominates (see *Fox et al*. [2012] for further details).

Two replicate sediment cores (10–20 cm) were collected for slurry incubations using acrylic tubes (7 cm inner diameter) from both low- and high-marsh zones in all C, HF, and XF plots (Figure 1). We devised the sampling scheme with the intention to evaluate both the effect of long-term fertilization and marsh elevation on nitrogen cycling. The cores in acrylic tubes with top and bottom sealed with rubber stoppers were kept cool with Techni-ICE[TM] ice packs during transportation to laboratory facilities. Samples were kept in a 4°C cold room until incubation experiments were performed the next day.

Three replicate sediment cores (~5 cm) from both low- and high-marsh zones in all treatment plots were collected for pore water nutrient determination using cutoff 60 mL syringes. These cores were transferred into 50 mL centrifuge tubes and stored on dry ice for transportation to laboratory facilities. In the lab, cores were thawed and immediately centrifuged at 4000 rpm for 15 min. The supernatants were filtered (0.7 μm nominal pore size, GF/F, Whatman, Maidstone, U.K.) and stored frozen in 15 mL centrifuge tubes until they were analyzed for nutrient concentrations.

2.2. Incubation Experiments

In total 24 sediment cores were collected for incubation experiments, with two cores from both marsh elevations (high and low) and six fertilization treatment plots (C1, C2, HF1, HF2, XF1, and XF2). The top 3 cm of each sediment core were homogenized after removing major roots. Approximately 1 g of homogenized sediment was aliquoted into 12 gas-tight 12 mL exetainers (Labco, High Wycombe, U.K.), and the headspace was flushed with a 20% oxygen/80% helium gas mixture at 3 psi for 5 min to minimize background N_2 while maintaining ambient oxygen concentrations. We then added 0.5 mL of 8 μM $^{15}NH_4^+$ made in artificial seawater [*Kester et al*., 1967] into six exetainers (Table 1). Three of the six incubations served as killed controls, which were treated with 0.5 mL of 2 M zinc chloride ($ZnCl_2$) before the addition of $^{15}NH_4^+$. A parallel set of six incubations with 0.5 mL of 2 μM $^{15}NO_3^-$ added were set up in the same manner Table 1. The ratio of sediment to added ^{15}N substrate solution (2:1 w/w) facilitated the even distribution of the added ^{15}N substrate by vigorous vortexing. All incubations were kept in the dark at room temperature (~21°C) for 1.5 h. The incubations were terminated by adding $ZnCl_2$. Both ^{15}N substrates and $ZnCl_2$ solutions were purged with the 20% O_2/80% He gas mixture to minimize the introduction of N_2.

Table 1. Summary of Parallel Incubations With ^{15}N-Labeled Substrates

^{15}N Substrate	Measured Product	Major Processes	Method	Reference
4 nmol of ^{15}NH$_4^+$	^{29}N$_2$	Coupled nitrification-denitrification	IRMS, direct sampling	*Rich et al.* [2008]
	^{15}NO$_3^-$	Nitrification	Denitrifier method	*Sigman et al.* [2001]
1 nmol of ^{15}NO$_3^-$	^{29}N$_2$	Denitrification	IRMS, direct sampling	*Rich et al.* [2008]
	^{15}NH$_4^+$	Dissimilatory nitrate reduction to ammonia (DNRA)	Oxidation with BrO$^-$ and reduction with azide	*Zhang et al.* [2007]

2.3. Measurement of Nutrient and Oxygen Concentrations

NH$_4^+$ and NO$_3^-$ concentrations in pore water samples were determined as described previously [*Ji et al.*, 2015]. In brief, NO$_3^-$ concentrations were measured in duplicate using a hot (90°C) acidified vanadium (III) reduction column coupled to a Teledyne Chemiluminescence NO/NO$_x$ Analyzer (Model 200E), with a detection limit of 0.5 μM [*Braman and Hendrix*, 1989; *Garside*, 1982]. NH$_4^+$ concentrations were measured colorimetrically in triplicate using the phenol-hypochlorite method [*Strickland and Parsons*, 1968] with a detection limit of 0.5 μM.

Dissolved inorganic nitrogen concentrations in incubated slurry sediments were measured after measuring N$_2$ in the headspace of incubation vials. To measure NO$_3^-$ concentrations in samples incubated with ^{15}NH$_4^+$, E-pure water (4 mL) was added to the incubation vials, which were capped and shaken at 200 rpm overnight in the dark. They were then centrifuged at 4000 rpm for 15 min, and the supernatant was transferred to 15 mL centrifuge tubes, which was centrifuged again at 4000 rpm for 15 min. The final supernatant was transferred to another set of 15 mL centrifuge tubes, which was immediately frozen and kept at −20°C. The NO$_3^-$ concentration in the supernatant was measured as described above.

To measure NH$_4^+$ concentrations in samples incubated with ^{15}NO$_3^-$, NH$_4^+$ was extracted from sediment samples by shaking the incubation vials at 200 rpm overnight after adding 4 mL of 2 N potassium chloride (KCl). The KCl extract was centrifuged at 4000 rpm for 15 min twice to remove any sedimentary material. The KCl extract was frozen immediately and kept at −20°C in 15 mL centrifuge tubes. The ZnCl$_2$ in the postincubation sediment slurries was inevitably introduced into the KCl extract and interfered with the colorimetric NH$_4^+$ measurement by precipitating white zinc oxide. Alternatively, the NH$_4^+$ concentration of the KCl extract was measured using fluorometry [*Holmes et al.*, 1999]. The presence of ZnCl$_2$ in samples did not interfere with the method or introduce an elevated blank, and the detection limit was 0.05 μM. The concentrations of KCl-exchangeable NH$_4^+$ were used to calculate rates below.

Depth profiles of oxygen concentrations in salt marsh sediments were measured using a Unisense oxygen microsensor (OX-500) with a sampling resolution of 500 μm. A two-point calibration of the microsensor was performed in the field before taking measurements with oxygen-free and oxygen-saturated water. Oxygen-free water was prepared by bubbling water with dry ice for 5 min; oxygen-saturated water was prepared by vigorously shaking water in a bottle to accelerate the equilibration of gas partial pressure between the water and the atmosphere. One high-resolution oxygen depth profile was collected at each fertilization treatment plot and marsh habitat. Oxygen concentrations were reported as percentage (%) saturation. Raw measurements of oxygen concentrations were corrected by setting the lowest reproducible value of oxygen concentration to 0%.

2.4. Determination of Net ^{15}NO$_3^-$ Production

The rate of ^{15}NO$_3^-$ production was measured by the increase in ^{15}NO$_3^-$ in sediment samples incubated with ^{15}NH$_4^+$. The δ^{15}N-NO$_3^-$ at both the start and end of incubations was determined using the denitrifier method [*Sigman et al.*, 2001]. A continuous flow purge and cryofocusing gas chromatography-mass spectrometry (Delta V Plus, Thermo Scientific) were used to measure the δ^{15}N-N$_2$O produced from the denitrifier method, with a precision of 0.5‰. Net production of ^{15}NO$_3^-$ normalized by sediment weight ($P_A^{15NO_3^-}$ in nmol g^{-1}) was calculated as

$$P_A^{15NO_3^-} = \frac{\text{Total NO}_3^- \times (\%^{15}\text{N}_{\text{End}} - \%^{15}\text{N}_0)}{w}$$

where Total NO_3^- is the total amount of NO_3^- in sediment slurries in nmol, w is the weight of the sediment in the incubation vial in grams, and $\%^{15}N_0$ and $\%^{15}N_{End}$ are the percentages of ^{15}N of NO_3^- at the start and end of the incubation, respectively. $P_A^{15_{NO_3^-}}$ was calculated only for incubations with $\%^{15}N_{End}$ that were significantly higher than $\%^{15}N_0$. The detection limit ranged from 0.0001 to 0.004 nmol g^{-1}, depending on the Total NO_3^- in the sample.

2.5. Determination of Net $^{15}NH_4^+$ Production

The production of $^{15}NH_4^+$ in incubations with $^{15}NO_3^-$ was measured using a method adapted from *Zhang et al.* [2007]. The $\delta^{15}N$-NH_4^+ at both the start and end of incubations was measured by first oxidizing NH_4^+ to NO_2^- using hypobromite (BrO^-) and then reducing NO_2^- to N_2O [*Zhang et al.*, 2007], with a precision of 0.5‰. The production of $^{15}NH_4^+$ normalized by sediment weight ($P_N^{15_{NH_4^+}}$ in nmol g^{-1}) was calculated as

$$P_N^{15_{NH_4^+}} = \frac{\text{Total } NH_4^+ \times (\%^{15}N_{End} - \%^{15}N_0)}{w}$$

where Total NH_4^+ is the total amount of KCl-exchangeable NH_4^+ in sediment slurries in nmol, w is the weight of the sediment in the incubation vial in grams, and $\%^{15}N_0$ and $\%^{15}N_{End}$ are the percentages of ^{15}N of NH_4^+ at the start and end of the incubation, respectively. $P_N^{15_{NH_4^+}}$ was calculated only for incubations with $\%^{15}N_{End}$ that were significantly higher than $\%^{15}N_0$. The production of $^{15}NH_4^+$ was not assayed in HF plots. The detection limit ranged from 0.004 to 0.46 nmol g^{-1} in C plots and 0.03 to 0.41 nmol g^{-1} in XF plots, depending on the Total NH_4^+ in the sample.

2.6. Determination of $^{29}N_2$ Production

The production of $^{29}N_2$ and $^{30}N_2$ (attributed to denitrification plus anammox) in each incubation vial was directly measured with a continuous flow isotope ratio mass spectrometer (Europa 20-20), in line with an automated gas preparation unit (Europa Scientific, ANCA-G Plus). Because the fraction of ammonium and nitrate labeled with ^{15}N (f_A and f_N, respectively) was low (Table S1 in the supporting information), no change in $^{30}N_2$ was detectable in any of the incubation vials. The amount of $^{29}N_2$ production normalized by sediment weight in incubations with $^{15}NO_3^-$ addition (P_N^{29} in nmol g^{-1}) was calculated as

$$P_N^{29} = \frac{\text{Total } N_2 \times (\%^{15}N_{End} - \%^{15}N_0)}{w}$$

where Total N_2 is the amount of N_2 in the headspace of the incubation vials in nmol, w is the weight of the sediment in the incubation vial in grams, and $\%^{15}N_0$ and $\%^{15}N_{End}$ are the percentages of ^{15}N of the N_2 at the start and end of the incubation, respectively. In the rest of this paper, letters "A" and "N" in subscripts are used to distinguish between incubations with $^{15}NH_4^+$ and $^{15}NO_3^-$ additions, respectively. P_N^{29} was calculated only for incubations with $\%^{15}N_{End}$ that were significantly higher than $\%^{15}N_0$. Depending on the Total N_2 in the sample, the detection limit ranged from 0.007 to 0.251 nmol g^{-1}, with a median of 0.033 nmol g^{-1}.

2.7. Rate Calculations With Numeric Modeling

The rates of nitrification (R_{NIT}), denitrification (R_{DN}), and DNRA (R_{DNRA}) were calculated using a box model constrained by the measured production of $^{29}N_2$, $^{15}NO_3^-$, and $^{15}NH_4^+$ (P_N^{29}, $P_A^{15_{NO_3^-}}$, and $P_N^{15_{NH_4^+}}$). Using one second as a time step, the model performed simulations for 5400 steps (1.5 h) using randomly generated rates with a uniform distribution. At the end of simulations, P_N^{29}, $P_A^{15_{NO_3^-}}$, and $P_N^{15_{NH_4^+}}$ calculated by the model were compared to measured values. The residuals between the model and measured P_N^{29}, $P_A^{15_{NO_3^-}}$, and $P_N^{15_{NH_4^+}}$ were calculated. The best model fit of R_{NIT}, R_{DN}, and R_{DNRA} was chosen by minimizing the sum of squares of the residuals. Anammox rates were assumed to contribute a negligible fraction of N_2 production [*Koop-Jakobsen and Giblin*, 2010]. Although nitrous oxide production was not included in
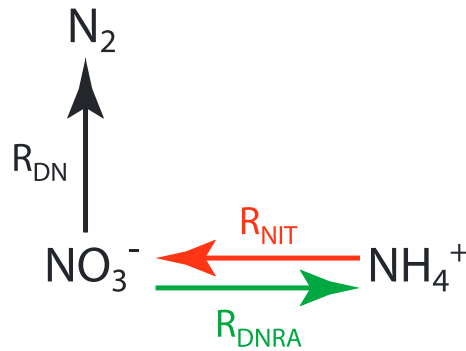
Figure 2. Nitrogen cycling processes in the box model included nitrification (R_{NIT}), denitrification (R_{DN}), and dissimilatory nitrate reduction to ammonium (R_{DNRA}).

this model, denitrification rates were unlikely underestimated, because nitrous oxide production rates were generally lower than or similar to consumption rates measured at the same site [Ji et al., 2015].

The model was implemented with the following N pools: $^{14/15}NH_4^+$, $^{14/15}NO_3^-$, and $^{29}N_2$ (Figure 2). At each time step T_n, each N pool was calculated as shown below.

Nitrification converts NH_4^+ to NO_3^-; DNRA converts NO_3^- to NH_4^+:

$$^{15}NH_4^+ \text{ at } T_n = {}^{15}NH_4^+ \text{ at } T_{n-1} - R_{NIT} \times f_A + R_{DNRA} \times f_N$$

$$^{14}NH_4^+ \text{ at } T_n = {}^{14}NH_4^+ \text{ at } T_{n-1} - R_{NIT} \times (1 - f_A) + R_{DNRA} \times (1 - f_N)$$

$$^{15}NO_3^- \text{ at } T_n = {}^{15}NO_3^- \text{ at } T_{n-1} + R_{NIT} \times f_A - R_{DNRA} \times f_N$$

$$^{14}NO_3^- \text{ at } T_n = {}^{14}NO_3^- \text{ at } T_{n-1} + R_{NIT} \times (1 - f_A) - R_{DNRA} \times (1 - f_N)$$

$^{29}N_2$ is produced from denitrification following binomial distribution:

$$^{29}N_2 \text{ at } T_n = R_{DN} \times 2 \times f_N \times (1 - f_N)$$

Calculate the cumulative $^{29}N_2$ production after T_n:

$$\text{Total } ^{29}N_2 \text{ after } T_n = \text{Total } ^{29}N_2 \text{ after } T_{n-1} + {}^{29}N_2 \text{ at } T_n$$

Calculate the cumulative $^{15}NO_3^-$ production after T_n:

$$\text{Total } P_A^{^{15}NO_3^-} = {}^{15}NO_3^- \text{ at } T_n - {}^{15}NO_3^- \text{ at } T_0$$

At the end of each time step, the fractions of NH_4^+ and NO_3^- labeled with ^{15}N (f_A and f_N, respectively) are recalculated for the next time step. Mass dependent fractionation effects were assumed to be negligible. Monte Carlo simulations ($n = 10,000$) were performed to calculate the standard deviations of R_{NIT}, R_{DN}, and R_{DNRA}. In each Monte Carlo simulation the following variables were randomly generated using a normal distribution: measured P_N^{29}, $P_A^{^{15}NO_3^-}$, $P_N^{^{15}NH_4^+}$, concentrations and $\%^{15}N$ of NH_4^+ and NO_3^- at T_0. The mean and standard deviation of these variables were calculated from triplicate measurements. After the first round of Monte Carlo simulations, a second round of Monte Carlo simulations ($n = 100$) was performed using R_{NIT}, R_{DN}, and R_{DNRA} randomly generated using a normal distribution, with the mean and standard deviation determined in the first round of simulations. Monte Carlo simulations with R_{NIT}, R_{DN}, and R_{DNRA} generated using a normal distribution were iterated until the standard deviations of R_{NIT}, R_{DN}, and R_{DNRA} approached asymptotes. Finally, the mean and standard deviation of R_{NIT}, R_{DN}, and R_{DNRA} generated from the second round of Monte Carlo simulations were calculated and reported. All calculations were performed in Matlab, and the code is included in the supporting information.

In samples from the high marsh of C plots, no P_N^{29} and $P_A^{^{15}NO_3^-}$ was detected, but $P_N^{^{15}NH_4^+}$ was significant, indicating only DNRA was active. In those cases, R_{DNRA} was calculated as

$$R_{DNRA} = \frac{\text{Total } NH_4^+ \times (\%^{15}N_{End} - \%^{15}N_0)}{w \times T \times f_N}$$

where T is the length of the incubation in hours, f_N is the fraction of nitrate labeled with ^{15}N at the start of the incubation, w is the weight of the sediment in the incubation vial in grams, and $\%^{15}N_0$ and $\%^{15}N_{End}$ are the percentages of ^{15}N and of NH_4^+ at the start and end of the incubation, respectively. R_{DNRA} was calculated only for incubations with $\%^{15}N_{End}$ that were significantly higher than $\%^{15}N_0$.
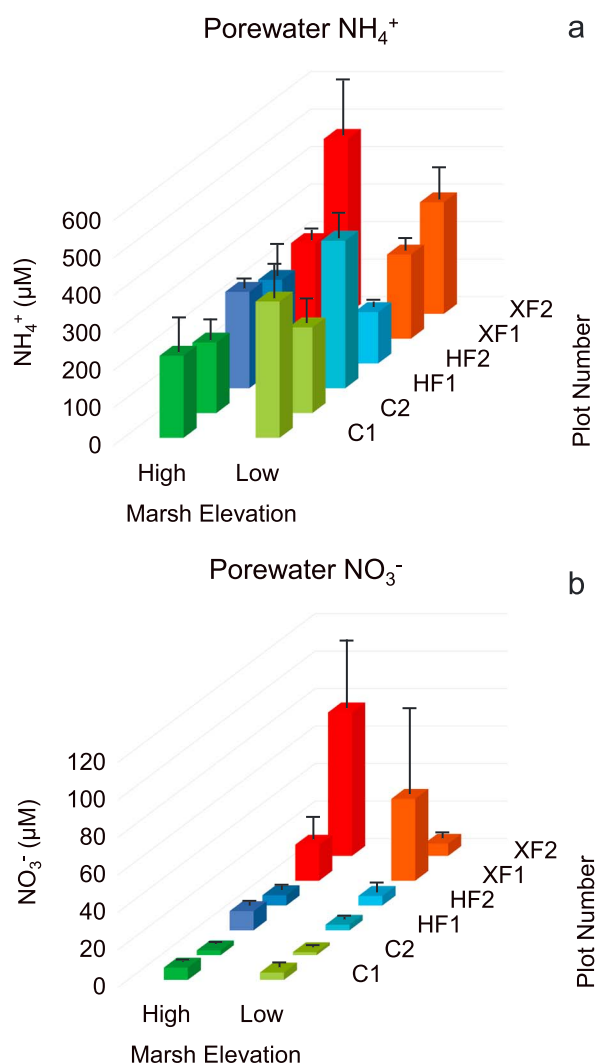
Figure 3. Concentrations (μM) of (a) ammonium (NH_4^+) and (b) nitrate (NO_3^-) in sediment pore water. Error bars represent standard deviations of measurements of three biological replicates. C: control; HF: high fertilization; XF: extra-high fertilization; High: high marsh; Low: low marsh.

2.8. Statistical Analysis

The differences between $\%^{15}N_{End}$ and $\%^{15}N_0$ ($n = 3$) were assessed for statistical significance using t test assuming unequal variance with two tails in Microsoft Excel. The same test was performed to evaluate the difference in nitrogen concentrations and transformation rates between treatment plots and the two marsh elevations. Specifically, in order to evaluate the effect of fertilization treatments, the nitrogen concentration ($n = 6$) and transformation rates ($n = 4$) in each marsh elevation (high or low) were compared pairwise (C versus HF, HF versus XF, and XF versus C). To assess the influence of marsh elevation, nitrogen concentration ($n = 3$) and transformation rates ($n = 2$) were compared between the high and low marshes within each fertilization treatment plot. The correlation coefficient between nitrification and denitrification rates was calculated in Matlab. A significance level of 0.05 was chosen for all tests.

3. Results

3.1. DIN and Oxygen Concentrations

Pore water NH_4^+ concentrations were similar among the different fertilization treatments (Figure 3a), except that pore water NH_4^+ concentration was higher in extra-high fertilization (XF) than in Control (C) in the high marsh (Table 2). The range of NH_4^+ concentrations in XF plots was the highest, but there was no clear increasing trend of NH_4^+ concentrations along the fertilization gradient. There was considerable variability among the three cores collected within the same treatment plot, as indicated by the error bars (Figure 3a). The fraction of $^{15}NH_4^+$ was low in all incubations, ranging from 0.4% to 1.5% (Table S1).

Pore water NO_3^- concentrations were low in C and high-fertilization (HF) plots (2–10 μM) and about an order of magnitude higher in XF plots except in XF2 low marsh (Figure 3b). These differences were statistically significant only in the high marsh (Table 2). No significant difference in NH_4^+ and NO_3^- concentrations was found between high- and low-marsh habitats, except the NO_3^- concentration in HF1 was higher in the high marsh than the low marsh (Table 3). The fraction of $^{15}NO_3^-$ ranged from 0.7% in the XF high marsh to 11% in the C high marsh (Table S1). NO_2^- concentration in pore water was below detection (0.05 μM).

Oxygen concentration decreased to zero by ~ 0.5 to 0.7 cm depth in the sediment in C, HF, and XF2 low marsh (Figure 4). The top 3 cm of the sediment were more oxygenated in XF high marshes and XF1 low marsh than in any other treatment and marsh habitats. Sediments in XF1 remained oxygenated throughout the top 3 cm of the sediment.

Table 2. Summary of t Test Results Comparing NH_4^+ Concentration ($[NH_4^+]$); NO_3^- Concentration ($[NO_3^-]$); and Rates of Nitrification, Denitrification, and DNRA at Both Marsh Elevations Between Fertilization Treatments ($n = 6$ for NH_4^+ and NO_3^- Concentration and $n = 4$ for Nitrogen Transformation Rates)[a]

	Marsh Elevation	$[NH_4^+]$	$[NO_3^-]$	Nitrification	Denitrification	DNRA
C versus HF	High	0.181	**0.030**	**0.041**	**0.033**	NA
	Low	0.343	0.283	0.142	0.120	NA
HF versus XF	High	0.057	**0.028**	**0.011**	***0.002***	NA
	Low	0.475	0.103	0.097	0.119	NA
XF versus C	High	**0.027**	**0.021**	***0.009***	***0.002***	0.083
	Low	0.255	0.093	**0.023**	0.079	0.112

[a]Bold fonts are used for p values < 0.05 and bold, italic fonts for p values < 0.01. NA: not applicable.

3.2. Nitrification Rates

Nitrification rates were below detection in the high marsh of Control (C) plots and were very low (0.6 – 2.4 nmol g^{-1} h^{-1}) in the low marsh of C plots (Figure 5a). Nitrification rates were highly variable in the high-fertilization (HF) plots, ranging from 1.3 to 12.8 nmol g^{-1} h^{-1} in the high marsh and from below detection to 34.0 nmol g^{-1} h^{-1} in the low marsh. In the high marsh, nitrification rates in HF plots were higher than in C plots (Table 2). In the extra-high fertilization (XF) plots, the range of nitrification rates was high (7.7–210.0 nmol g^{-1} h^{-1}) and rates were generally higher than those in HF and C plots in the high marsh (Table 2). Nitrification rates in XF1 Low 1 was the lowest among all samples from XF plots ($p < 0.001$). No difference in nitrification rates was found between high and low marshes (Table 3), mainly due to the high variability within each marsh habitat (Figure 5a).

3.3. Denitrification Rates

Denitrification was not detected in the high marsh of control (C) plots, and rates were very low (0.5– 1.2 nmol g^{-1} h^{-1}) in the low marsh of C plots (Figure 5b). In the high-fertilization (HF) plots, denitrification rates were detected in both high and low marshes, ranging from 0 to 5.4 nmol g^{-1} h^{-1}. In the high-marsh habitat, denitrification rates were higher in HF plots than C plots and were highest (21.7–34.3 nmol g^{-1} h^{-1}) in extra-high fertilization (XF) plots (Table 2). In the low marsh of XF plots, denitrification rates were highly variable, spanning a range of 1.5 to 22.0 nmol g^{-1} h^{-1}. The lowest denitrification rate in XF plots was found in XF1 Low 1. There was a significant linear correlation between nitrification and denitrification rates ($R = 0.82$, and $p < 0.001$; Figure 6).

3.4. DNRA Rates

The pattern displayed by DNRA rates was essentially the opposite of denitrification rates (Figure 5c). No DNRA was detected in extra-high fertilization (XF) plots except in XF1 Low 1, where DNRA rate was 6.7 nmol g^{-1} h^{-1}. DNRA rates were high in control (C) plots and showed large variability (0–42.1 nmol g^{-1} h^{-1}) within each plot and marsh elevation. DNRA was not measured in the HF plots because the difference in oxygen, NH_4^+ and NO_3^- concentrations, nitrification, and denitrification rates were not significant between C and high-fertilization (HF) plots.

Table 3. Summary of t Test Results Comparing NH_4^+ Concentration ($[NH_4^+]$); NO_3^- Concentration ($[NO_3^-]$); and Rates of Nitrification, Denitrification, and DNRA Between High and Low Marshes ($n = 3$ for NH_4^+ and NO_3^- Concentration and $n = 2$ for Nitrogen Transformation Rates)[a]

Treatment Plot	$[NH_4^+]$	$[NO_3^-]$	Nitrification	Denitrification	DNRA
C1	0.132	0.191	0.290	0.262	0.727
C2	0.465	0.301	0.500	0.500	0.623
HF1	0.061	**0.013**	0.350	0.204	NA
HF2	0.222	0.917	0.155	0.337	NA
XF1	0.289	0.453	0.130	0.477	0.500
XF2	0.181	0.078	0.335	0.146	1.000

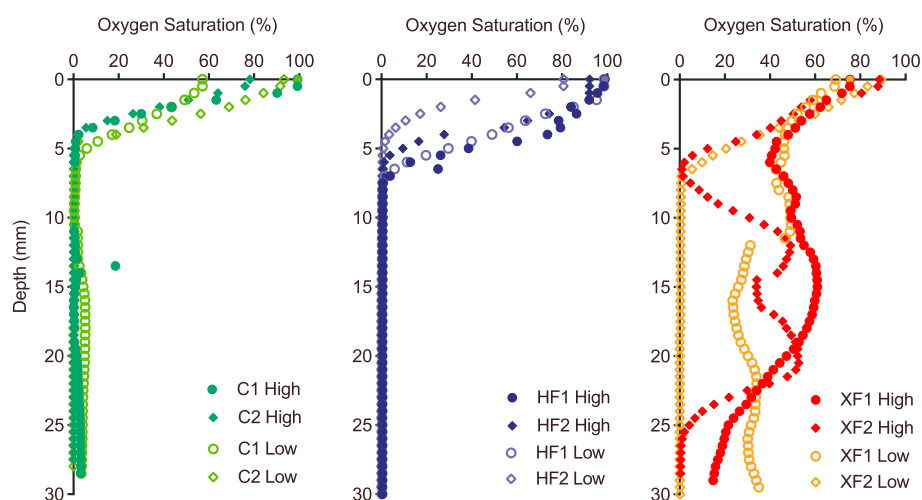[a]Bold fonts are used for p values < 0.05. NA: not applicable.

Figure 4. Depth profiles of oxygen in the top 30 mm of salt marsh sediments. C: Control; HF: high fertilization; XF: extra-high fertilization; High: high marsh; and Low: low marsh.

3.5. NO$_3^-$ Removal Versus Retention

DNRA accounted for all NO$_3^-$ reduction in control (C) high marsh and nearly all NO$_3^-$ reduction in C low marsh, while denitrification was the dominant NO$_3^-$ reduction pathway in most of the XF plots except in XF1 Low 1 (Figure 5). DNRA was not assayed in HF plots.

4. Discussion

The use of oxic headspace during incubations in this study distinguishes our experimental results from previous investigations in which the potential of anaerobic processes were assessed under anoxia [e.g., *Risgaard-Petersen et al.*, 2004; *Rich et al.*, 2008]. The presence of oxygen in the incubations allowed for, and possibly stimulated nitrification, which produced substrates for denitrification and DNRA. In the plots where highest denitrification rates were detected, the ambient concentration of nitrate was quite high, so denitrification was probably not limited by substrate supplied from nitrification. Nonetheless, nitrification and denitrification are usually tightly coupled in salt marsh sediments [*Hamersley and Howes*, 2005; *Patrick and Reddy*, 1976], often aided by the transport of oxygen into anoxic depths via the aerenchyma of *S. alterniflora* [*Arenovski and Howes*, 1992]. On the other hand, denitrification and DNRA were potentially inhibited in our incubations because sediment homogenization disrupted in situ oxygen gradients and exposed anaerobic microorganisms to oxygen. Therefore, rates determined in this study may not be equivalent to in situ rates, even though the addition of ^{15}N labeled substrates at true tracer levels minimized stimulation. Denitrification has been extensively studied in coastal marine sediments, including salt marshes, but DNRA has received less attention as a NO$_3^-$ reduction pathway. This study determined rates of nitrification, denitrification, and DNRA simultaneously and examined the effect of long-term fertilization on salt marsh sediment N cycling.

4.1. The Effect of Long-Term Fertilization on the Great Sippewissett Marsh

The Great Sippewissett Marsh is limited by N as shown by a comprehensive study on its N budget [*Valiela and Teal*, 1979]. In the experimental plots receiving long-term fertilization, enhanced primary production, nutrient retention, organic N content, N$_2$ production, and nitrous oxide production have been documented [*Valiela et al.*, 1973, 1975; *Hamersley and Howes*, 2005; *Brin et al.*, 2010; *Kinney and Valiela*, 2013; *Uldahl*, 2011; *Ji et al.*, 2015]. These previous studies showed that the various effects of long-term fertilization were usually more pronounced in extra-high-fertilization (XF) plots than in high-fertilization (HF) plots. Vegetation cover has also been altered by long-term fertilization, notably the succession of *D. spicata* after *S. alterniflora* in the high marsh of XF plots [*Fox et al.*, 2012]. The high marsh of XF plots has also been elevated due to high accretion rates [*Fox et al.*, 2012], resulting in shorter periods of tidal inundation and drier sediment compared to those of control (C) plots. This is also reflected by the oxygen depth profile in the high marsh of XF plots, which was at about 50% saturation between 1 and 2.5 cm depth, an interval that was completely anoxic in C
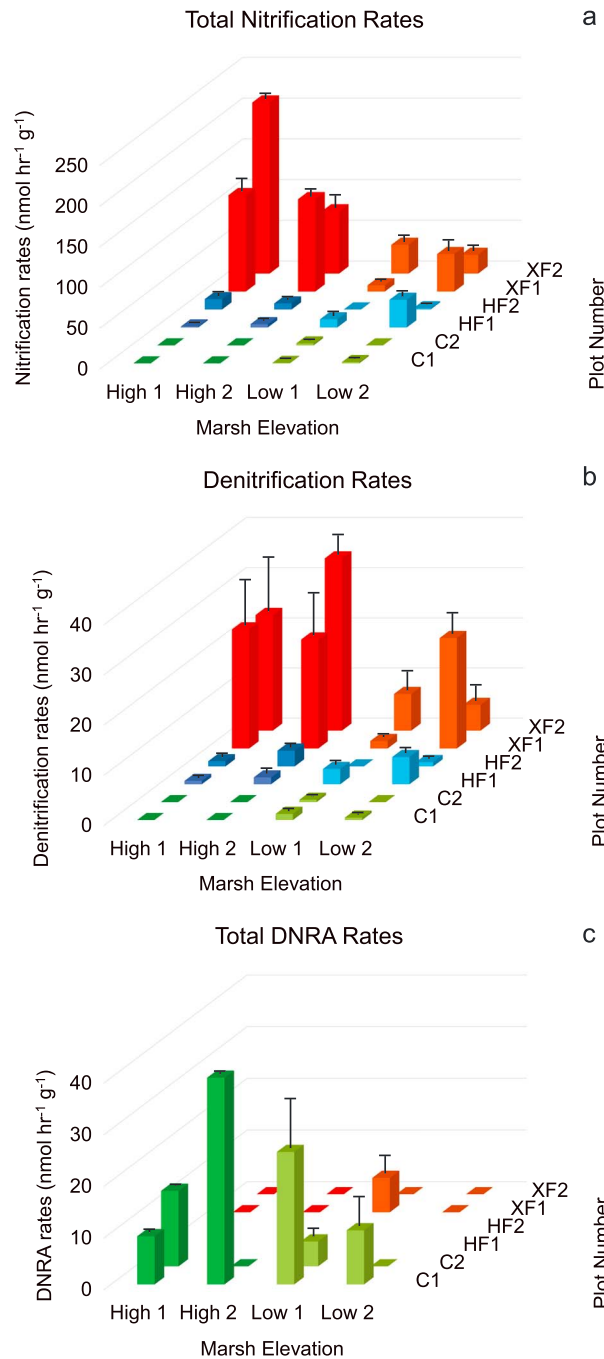
Figure 5. Rates of (a) total nitrification, (b) denitrification, and (c) dissimilatory nitrate reduction to ammonia (DNRA) computed using our numerical model. Error bars represent standard deviations of rates calculated by Monte Carlo simulations ($n = 10{,}000$). C: Control; HF: high fertilization; XF: extra-high fertilization; High: high marsh; and Low: low marsh. DNRA rates were not assayed in HF plots.

and HF plots (Figure 4). Long-term fertilization did not increase the abundance of ammonia oxidizers [*Peng et al.*, 2013], suggesting that the per-cell ammonia oxidation rate was higher in fertilized plots. This response by the ammonia-oxidizing population was likely a result of more oxidized sediments due to long-term fertilization (Figure 4) [*Howes et al.*, 1986].

4.2. Denitrification

Denitrification rates determined in both fertilized and unfertilized plots were comparable to earlier measurements in the same experimental plots [*Kaplan et al.*, 1977, 1979; *Hamersley and Howes*, 2005]. In Control (C) plots, denitrification rates were low in the low marsh and were not detected in the high marsh (Figure 5c). This is consistent with the previous finding of low or no rates of N_2 production in the high marsh of C plots [*Hamersley and Howes*, 2005; *Kaplan et al.*, 1979]. Elevated nitrification rates probably supported the denitrification in HF plots (Figure 5a), since the applied fertilizer hydrolyzed into NH_4^+ or organic nitrogen. Denitrification rates were the highest in extra-high fertilization (XF) plots and were similar to those measured in the same XF high marsh 10 years earlier using in situ $^{15}NH_4^+$ injection technique and mass balance calculations [*Hamersley and Howes*, 2005]. Such enhanced denitrification rates in fertilized plots contributed significantly toward fixed N removal and maintaining relatively low levels of N export. A previous study showed that although dissolved inorganic nitrogen export was enhanced in XF plots, export of added N was $< 7\%$ for all treatment plots at Great Sippewissett Marsh [*Brin et al.*, 2010].

Elevated N removal via denitrification as a result of fertilization has been reported previously [*Drake et al.*, 2009; *Hamersley and Howes*, 2005]. Assuming that the organic carbon content of sediments in these experimental plots have not changed significantly since it was last reported [*Hamersley and Howes*, 2005], the organic carbon content was unlikely limiting denitrification because it was high in all plots. Denitrification
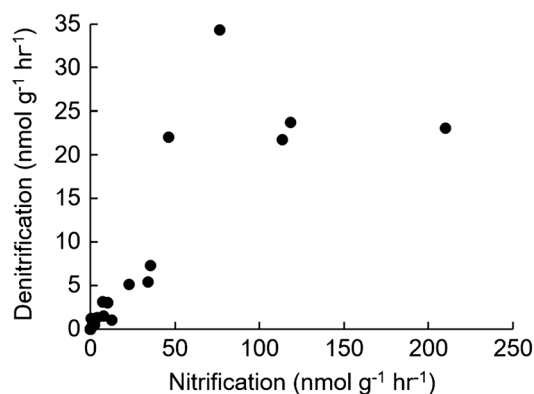
Figure 6. The positive correlation between rates of denitrification and nitrification ($R = 0.82$, and $p < 0.001$).

was likely limited by NO_3^- availability. Indeed, NO_3^- concentrations in XF plots were significantly higher than those in HF and C plots (Figure 3b). High NO_3^- concentrations in XF plots probably resulted from high nitrification rates. Therefore, nitrification and denitrification were tightly coupled, as indicated by a positive correlation between nitrification and denitrification rates ($R = 0.82$, and $p < 0.001$; Figure 6). This is consistent with previous reports of tightly coupled nitrification and denitrification in estuarine sediments [e.g., *Jenkins and Kemp*, 1984; *White and Howes*, 1994; *An and Joye*, 2001]. The oxic headspace in our incubations allowed NO_3^- production via nitrification, thereby providing substrates for denitrification. On the other hand, high oxygen consumption rates probably established sharp oxygen gradients and anoxic microsites in the sediment slurry, allowing the activity of anaerobic processes. Since nitrification-derived NO_3^- fueled denitrification, only small amounts of $^{15}NO_3^-$ (<10% of ambient levels in most cases; Table S1) were required for incubations, minimizing potential stimulation of denitrification rates.

Because the experimental design used here precluded independent quantification of anammox rates, the total rates of N loss were most likely higher than those reported here from denitrification alone. However, anammox has been shown to account for < 3% of total N loss from salt marsh sediments [*Koop-Jakobsen and Giblin*, 2009], so the total rates of N loss can be approximated with denitrification rates.

4.3. DNRA

In contrast to denitrification, DNRA, which retains fixed N within the sediment, was the dominant NO_3^- reduction pathway in control (C) plots and was not detected in extra-high fertilization (XF) plots. The relative importance of DNRA and denitrification in NO_3^- reduction is theoretically controlled by both energetics and kinetics [*Tiedje et al.*, 1982]. Because the Gibbs free energy per NO_3^- reduced from DNRA is slightly higher than that from denitrification, *Tiedje et al.* [1982] predicted that when NO_3^- is limiting, DNRA should be favored over denitrification. A recent modeling study based on the same idea also predicted a shift from denitrification to DNRA (and finally to anammox) as the substrate carbon/NO_3^- ratio increases [*Algar and Vallino*, 2014]. This prediction has been supported by both field and culture studies. Incubation experiments with salt marsh sediments at various NO_3^- concentrations showed a gradual shift from DNRA dominating low NO_3^- conditions to denitrification dominating high NO_3^- conditions [*King and Nedwell*, 1985]. Growth experiments with *Paracoccus denitrificans* and *Pseudomonas stutzeri* (which reduce NO_3^- to N_2) and *Wolinella succinogenes* and *Sulfurospirillum deleyianum* (which reduce NO_3^- to NH_4^+) showed that growth yields from denitrification were lower compared to those from DNRA [*Strohm et al.*, 2007]. While carbon/NO_3^- ratio appeared to be positively correlated with the relative importance of DNRA, a recent field study showed that high organic carbon is a prerequisite for DNRA to be favored over denitrification [*Hardison et al.*, 2015].

In the Great Sippewissett Marsh, organic carbon content was only slightly higher in XF than in Control (C) plots (3.9 v. 3.1 mmol m^{-3}) [*Hamersley and Howes*, 2005]. Hence, the more than tenfold higher NO_3^- concentration in XF than C plots means higher carbon/NO_3^- ratio in C plots, which is consistent with the dominance of DNRA in C plots. Direct rate measurements of DNRA in other salt marsh ecosystems provide further evidence supporting the control of carbon/NO_3^- ratio on the significance of DNRA relative to denitrification. Salt marsh sediments in Breton Sound, Louisiana, removed two thirds of added $^{15}NO_3^-$ (2 mg L^{-1}) in the overlying water during a 3 month incubation, suggesting a small role of DNRA relative to denitrification under elevated NO_3^- [*VanZomeren et al.*, 2012]. Whole-core incubations at the Plum Island LTER found that DNRA in fertilized marsh (29%) accounted for a smaller percentage of the total NO_3^- reduction than in the reference

marsh (41%), although DNRA rates were sixfold higher in fertilized than unfertilized salt marsh sediments [*Koop-Jakobsen and Giblin*, 2010]. It is worth noting that the fertilization experiment at the Plum Island LTER adopted an ecosystem scale (~60,000 m^2 of marshlands) approach, which pumps NO_3^- into the flooding water of every tide during the growing season to reach a water column concentration of 70 µmol N L^{-1} [*Deegan et al.*, 2007]. Moreover, the total N loading and fertilization duration (4 years) at Plum Island LTER experimental marshes was an order of magnitude lower than the HF and XF plots in Great Sippewissett Marsh. In particular, pore water NO_3^- concentrations in marsh sediments at Plum Island LTER were not different between fertilized and reference marshes [*Koop-Jakobsen and Giblin*, 2010]. Therefore, the modest shift between fertilized and reference marshes in the relative contribution of DNRA to NO_3^- reduction in the Plum Island LTER experiments may be attributed to the relatively small annual N loading compared to other fertilization experiments [*Deegan et al.*, 2007]. Another recent study at Plum Island LTER suggested that the relative importance of DNRA was greater in the tidal creek of fertilized than reference marshes [*Vieillard and Fulweiler*, 2012]. However, the mass balance approach used in this study assumed that denitrification and DNRA were the only two NO_3^- uptake pathways and did not include possible NO_3^- assimilation by benthic algae and microorganisms, which likely accounted for part of the NO_3^- uptake [*Koop-Jakobsen and Giblin*, 2010]. By contrast, direct measurements in the same tidal creeks found no change in the percentage of DNRA between fertilized and reference marshes, despite the tenfold higher NO_3^- levels in the tidal creek of fertilized than reference marshes [*Koop-Jakobsen and Giblin*, 2010]. This suggests that either the labile carbon in the tidal creek of fertilized marshes was also tenfold higher than that of reference marshes or there may be other controls on the relative importance of DNRA in addition to carbon/NO_3^- ratio.

Among other environmental variables, temperature and sulfide levels have been suggested to be important in determining the relative contribution of different NO_3^- reduction pathways [*Brunet and Garcia-Gil*, 1996; *Ogilvie et al.*, 1997]. High temperature was suggested to favor DNRA, as shown by a study in a tropical estuary [*Dong et al.*, 2011]. However, all DNRA studies in salt marshes mentioned above were in temperate zones, where temperature is unlikely to be a significant factor in regulating the relative importance of DNRA. Sulfide concentration is another variable that controls the activity of DNRA and denitrification. High sulfide concentrations could inhibit the last step of denitrification, but not DNRA [*Ogilvie et al.*, 1997; *An and Gardner*, 2002], suggesting that DNRA may be favored in sediments with high sulfide concentrations. Since much of the marsh area in the XF plots remained oxic through the top 3 cm of sediments, there was likely much lower sulfide concentrations in the XF plots compared to the C plots, supporting the notion that sulfide may play a role in regulating the relative proportion of these rates.

4.4. The Influence of Marsh Elevation

Besides the effect of long-term fertilization, the influence of marsh elevation on dissimilatory nitrate reduction pathways was also assessed in our study. Because of the high variability between the duplicate cores collected within the same marsh elevation and experimental plot, there was no significant difference in nitrogen concentrations or transformation rates between high- and low-marsh habitats with only one exception (Table 3). However, all significant differences in nitrogen concentrations and transformation rates between fertilization treatments were only found in high-marsh habitats with only one exception (Table 2). This indicates a compounded effect of fertilization and marsh elevation. The maximum elevation in extra-high fertilization (XF) high-marsh plots was 28 cm greater than in Control (C) high-marsh plots [*Fox et al.*, 2012], which directly translated into shorter amount of inundation time during high tides in the XF than the C plots. Longer period of exposure to the atmosphere in XF high marsh was clearly reflected by the oxygen profiles compared to C plots (Figure 4). Moreover, XF high marsh is subject to less physical energy to export detritus than C high marsh [*Odum and Heywood*, 1978]. On the other hand, there was no difference in marsh elevation between fertilization plots in low marshes, where tidal exchange largely eliminates the difference in carbon and nitrogen contents due to fertilization [*Brin et al.*, 2010]. Therefore, marsh elevation has an indirect but nontrivial influence on the effect long-term fertilization on N cycling in salt marsh sediments.

5. Conclusions

The incubations performed with Great Sippewissett Marsh sediments suggested that long-term fertilization shifted the dominant NO_3^- reduction pathway from DNRA to denitrification. The contribution of DNRA to total NO_3^- reduction relative to denitrification largely depends on carbon/NO_3^- ratio in the sediment. Salt marsh

sediments have a large potential to remove fixed N, and a significant portion of N loading arriving from upstream will be intercepted before entering the coastal ocean. Nonetheless, salt marshes cannot remove N infinitely [*Drake et al.*, 2009]. While salt marsh ecosystems can respond to anthropogenic N loading with a greater denitrification potential, it should be noted that long-term fertilization has resulted in loss of salt marsh area around the world [*Deegan et al.*, 2012]. Therefore, it is critical to protect salt marshes by reducing N loading.

References

Algar, C. K., and J. J. Vallino (2014), Predicting microbial nitrate reduction pathways in coastal sediments, *Aquat. Microb. Ecol.*, *71*(3), 223–238, doi:10.3354/ame01678.

An, S. M., and W. S. Gardner (2002), Dissimilatory nitrate reduction to ammonium (DNRA) as a nitrogen link, versus denitrification as a sink in a shallow estuary (Laguna Madre/Baffin Bay, Texas), *Mar. Ecol. Prog. Ser.*, *237*, 41–50, doi:10.3354/Meps237041.

An, S. M., and S. B. Joye (2001), Enhancement of coupled nitrification-denitrification by benthic photosynthesis in shallow estuarine sediments, *Limnol. Oceanogr.*, *46*(1), 62–74, doi:10.4319/lo.2001.46.1.0062.

Arenovski, A. L., and B. L. Howes (1992), Lacunal allocation and gas transport capacity in the salt marsh grass *Spartina alterniflora*, *Oecologia*, *90*(3), 316–322, doi:10.1007/Bf00317687.

Braman, R. S., and S. A. Hendrix (1989), Nanogram nitrite and nitrate determination in environmental and biological materials by vanadium (III) reduction with chemiluminescence detection, *Anal. Chem.*, *61*(24), 2715–2718, doi:10.1021/ac00199a007.

Brin, L. D., I. Valiela, D. Goehringer, and B. Howes (2010), Nitrogen interception and export by experimental salt marsh plots exposed to chronic nutrient addition, *Mar. Ecol. Prog. Ser.*, *400*, 3–17, doi:10.3354/meps08460.

Brin, L. D., A. E. Giblin, and J. J. Rich (2015), Effects of experimental warming and carbon addition on nitrate reduction and respiration in coastal sediments, *Biogeochemistry*, *125*(1), 81–95, doi:10.1007/s10533-015-0113-4.

Brunet, R. C., and L. J. Garcia-Gil (1996), Sulfide-induced dissimilatory nitrate reduction to ammonia in anaerobic freshwater sediments, *FEMS Microb. Ecol.*, *21*(2), 131–138, doi:10.1111/j.1574-6941.1996.tb00340.x.

Burgin, A. J., and S. K. Hamilton (2007), Have we overemphasized the role of denitrification in aquatic ecosystems? A review of nitrate removal pathways, *Front. Ecol. Environ.*, *5*(2), 89–96.

Dalsgaard, T., B. Thamdrup, and D. E. Canfield (2005), Anaerobic ammonium oxidation (anammox) in the marine environment, *Res. Microbiol.*, *156*(4), 457–464, doi:10.1016/j.resmic.2005.01.011.

Deegan, L. A., et al. (2007), Susceptibility of salt marshes to nutrient enrichment and predator removal, *Ecol. Appl.*, *17*, S42–S63, doi:10.1890/06-0452.1.

Deegan, L. A., D. S. Johnson, R. S. Warren, B. J. Peterson, J. W. Fleeger, S. Fagherazzi, and W. M. Wollheim (2012), Coastal eutrophication as a driver of salt marsh loss, *Nature*, *490*(7420), 388–392, doi:10.1038/nature11533.

Dong, L. F., M. Naqasima Sobey, C. J. Smith, I. Rusmana, W. Phillips, A. Stott, A. M. Osborn, and D. B. Nedwell (2011), Dissimilatory reduction of nitrate to ammonium, not denitrification or anammox, dominates benthic nitrate reduction in tropical estuaries, *Limnol. Oceanogr.*, *56*(1), 279–291, doi:10.4319/lo.2011.56.1.0279.

Drake, D. C., B. J. Peterson, K. A. Galvan, L. A. Deegan, C. Hopkinson, J. M. Johnson, K. Koop-Jakobsen, L. E. Lemay, and C. Picard (2009), Salt marsh ecosystem biogeochemical responses to nutrient enrichment: A paired ^{15}N tracer study, *Ecology*, *90*(9), 2535–2546, doi:10.1890/08-1051.1.

Duarte, C. M., J. J. Middelburg, and N. Caraco (2005), Major role of marine vegetation on the oceanic carbon cycle, *Biogeosciences*, *2*(1), 1–8.

Engstrom, P., T. Dalsgaard, S. Hulth, and R. C. Aller (2005), Anaerobic ammonium oxidation by nitrite (anammox): Implications for N_2 production in coastal marine sediments, *Geochim. Cosmochim. Acta*, *69*(8), 2057–2065, doi:10.1016/j.gca.2004.09.032.

Fox, L., I. Valiela, and E. L. Kinney (2012), Vegetation cover and elevation in long-term experimental nutrient-enrichment plots in Great Sippewissett Salt Marsh, Cape Cod, Massachusetts: Implications for eutrophication and sea level rise, *Estuar. Coast.*, *35*(2), 445–458, doi:10.1007/s12237-012-9479-x.

Garside, C. (1982), A Chemiluminescent technique for the determination of nanomolar concentrations of nitrate and nitrite in seawater, *Mar. Chem.*, *11*(2), 159–167, doi:10.1016/0304-4203(82)90039-1.

Giblin, A., C. Tobias, B. Song, N. Weston, G. Banta, and V. Rivera-Monroy (2013), The importance of dissimilatory nitrate reduction to ammonium (DNRA) in the nitrogen cycle of coastal ecosystems, *Oceanography*, *26*(3), 124–131, doi:10.5670/oceanog.2013.54.

Groffman, P. M., M. A. Altabet, J. K. Böhlke, K. Butterbach-Bahl, M. B. David, M. K. Firestone, A. E. Giblin, T. M. Kana, L. P. Nielsen, and M. A. Voytek (2006), Methods for measuring denitrification: Diverse approaches to a difficult problem, *Ecol. Appl.*, *16*, 2091–2122, doi:10.1890/1051-0761(2006)016[2091:MFMDDA]2.0.CO;2.

Hamersley, M. R., and B. L. Howes (2005), Coupled nitrification-denitrification measured in situ in a *Spartina alterniflora* marsh with a $^{15}NH_4^+$ tracer, *Mar. Ecol. Prog. Ser.*, *299*, 123–135, doi:10.3354/meps299123.

Hardison, A. K., C. K. Algar, A. E. Giblin, and J. J. Rich (2015), Influence of organic carbon and nitrate loading on partitioning between dissimilatory nitrate reduction to ammonium (DNRA) and N_2 production, *Geochim. Cosmochim. Acta*, *164*, 146–160, doi:10.1016/j.gca.2015.04.049.

Holmes, R. M., A. Aminot, R. Kerouel, B. A. Hooker, and B. J. Peterson (1999), A simple and precise method for measuring ammonium in marine and freshwater ecosystems, *Can. J. Fish. Aquat. Sci.*, *56*(10), 1801–1808, doi:10.1139/cjfas-56-10-1801.

Howes, B. L., J. W. H. Dacey, and D. D. Goehringer (1986), Factors controlling the growth form of *Spartina alterniflora*: Feedbacks between aboveground production, sediment oxidation, nitrogen and salinity, *J. Ecol.*, *74*(3), 881–898, doi:10.2307/2260404.

Jenkins, M. C., and W. M. Kemp (1984), The coupling of nitrification and denitrification in two estuarine sediments, *Limnol. Oceanogr.*, *29*(3), 609–619, doi:10.4319/lo.1984.29.3.0609.

Ji, Q., A. R. Babbin, X. Peng, J. L. Bowen, and B. B. Ward (2015), Nitrogen substrate-dependent nitrous oxide cycling in salt marsh sediments, *J. Mar. Res.*, *73*, 71–92, doi:10.1357/002224015815848820.

Kana, T. M., M. B. Sullivan, J. C. Cornwell, and K. M. Groxzkowski (1998), Denitrification in estuarine sediments determined by membrane inlet mass spectrometry, *Limnol. Oceanogr.*, *43*(2), 334–339, doi:10.4319/lo.1998.43.2.0334.

Kaplan, W., I. Valiela, and J. M. Teal (1979), Denitrification in a salt marsh ecosystem, *Limnol. Oceanogr.*, *24*(4), 726–734, doi:10.4319/lo.1979.24.4.0726.

Kaplan, W. A., J. M. Teal, and I. Valiela (1977), Denitrification in salt marsh sediments: Evidence for seasonal temperature selection among populations of denitrifiers, *Microb. Ecol.*, *3*(3), 193–204, doi:10.1007/Bf02010617.

Kester, D. R., I. W. Duedall, D. N. Connors, and R. M. Pytkowicz (1967), Preparation of artificial seawater, *Limnol. Oceanogr.*, *12*(1), 176–179, doi:10.4319/lo.1967.12.1.0176.

King, D., and D. B. Nedwell (1985), The influence of nitrate concentration upon the end-products of nitrate dissimilation by bacteria in anaerobic salt marsh sediment, *FEMS Microbiol. Ecol.*, *31*(1), 23–28, doi:10.1111/j.1574-6968.1985.tb01127.x.

Kinney, E. L., and I. Valiela (2013), Changes in δ^{15}N in salt marsh sediments in a long-term fertilization study, *Mar. Ecol. Prog. Ser.*, *477*, 41–52, doi:10.3354/meps10147.

Koop-Jakobsen, K., and A. E. Giblin (2009), Anammox in tidal marsh sediments: The role of salinity, nitrogen loading, and marsh vegetation, *Estuar. Coast.*, *32*(2), 238–245, doi:10.1007/s12237-008-9131-y.

Koop-Jakobsen, K., and A. E. Giblin (2010), The effect of increased nitrate loading on nitrate reduction via denitrification and DNRA in salt marsh sediments, *Limnol. Oceanogr.*, *55*(2), 789–802, doi:10.4319/lo.2009.55.2.0789.

Moller, I., et al. (2014), Wave attenuation over coastal salt marshes under storm surge conditions, *Nat. Geosci.*, *7*(10), 727–731, doi:10.1038/Ngeo2251.

Nishio, T., I. Koike, and A. Hattori (1983), Estimates of denitrification and nitrification in coastal and estuarine sediments, *Appl. Environ. Microbiol.*, *45*(2), 444–450.

Odum, W. E., and M. A. Heywood (1978), Decomposition of intertidal freshwater marsh plants, in *Freshwater Wetlands: Ecological Processes and Management Potential*, edited by R. E. Good et al., pp. 89–98, Academic Press, New York.

Ogilvie, B. G., M. Rutter, and D. B. Nedwell (1997), Selection by temperature of nitrate-reducing bacteria from estuarine sediments: Species composition and competition for nitrate, *FEMS Microbiol. Ecol.*, *23*(1), 11–22, doi:10.1111/j.1574-6941.1997.tb00386.x.

Patrick, W. H., and K. R. Reddy (1976), Nitrification-denitrification reactions in flooded soils and water bottoms: Dependence on oxygen supply and ammonium diffusion, *J. Environ. Qual.*, *5*(4), 469–472.

Peng, X., E. Yando, E. Hildebrand, C. Dwyer, A. Kearney, A. Waciega, I. Valiela, and A. E. Bernhard (2013), Differential responses of ammonia-oxidizing archaea and bacteria to long-term fertilization in a New England salt marsh, *Frontiers Microbiol.*, *3*, doi:10.3389/fmicb.2012.00445.

Rich, J. J., O. R. Dale, B. Song, and B. B. Ward (2008), Anaerobic ammonium oxidation (anammox) in Chesapeake Bay sediments, *Microbiol. Ecol.*, *55*, 311–320, doi:10.1007/s00248-007-9277-3.

Risgaard-Petersen, N., L. P. Nielsen, S. Rysgaard, T. Dalsgaard, and R. L. Meyer (2003), Application of the isotope pairing technique in sediments where anammox and denitrification coexist, *Limnol. Oceanogr. Meth.*, *1*, 63–73, doi:10.4319/lom.2003.1.63.

Risgaard-Petersen, N., R. L. Meyer, M. Schmid, M. S. M. Jetten, A. Enrich-Prast, S. Rysgaard, and N. P. Revsbech (2004), Anaerobic ammonium oxidation in an estuarine sediment, *Aquat. Microbiol. Ecol.*, *36*(3), 293–304, doi:10.3354/ame036293.

Rysgaard, S., N. Risgaard-Petersen, S. Niels Peter, J. Kim, and N. Lars Peter (1994), Oxygen regulation of nitrification and denitrification in sediments, *Limnol. Oceanogr.*, *39*(7), 1643–1652, doi:10.4319/lo.1994.39.7.1643.

Seitzinger, S., S. Nixon, M. E. Q. Pilson, and S. Burke (1980), Denitrification and N$_2$O production in near-shore marine sediments, *Geochim. Cosmochim. Acta*, *44*(11), 1853–1860, doi:10.1016/0016-7037(80)90234-3.

Sigman, D. M., K. L. Casciotti, M. Andreani, C. Barford, M. Galanter, and J. K. Bohlke (2001), A bacterial method for the nitrogen isotopic analysis of nitrate in seawater and freshwater, *Anal. Chem.*, *73*(17), 4145–4153, doi:10.1021/Ac010088e.

Song, G. D., S. M. Liu, H. Marchant, M. M. M. Kuypers, and G. Lavik (2013), Anammox, denitrification and dissimilatory nitrate reduction to ammonium in the East China Sea sediment, *Biogeosciences*, *10*(11), 6851–6864, doi:10.5194/bg-10-6851-2013.

Sousa, A. I., A. I. Lillebo, I. Cacador, and M. A. Pardal (2008), Contribution of *Spartina maritima* to the reduction of eutrophication in estuarine systems, *Environ. Pollut.*, *156*(3), 628–635, doi:10.1016/j.envpol.2008.06.022.

Strickland, J. D. H., and T. R. Parsons (1968), *A Practical Handbook of Seawater Analysis, Bulletin of Fisheries Research Board of Canada*, *167*, Ottawa, Canada, Fisheries Research Board of Canada, 311 pp.

Strohm, T. O., B. Griffin, W. G. Zumft, and B. Schink (2007), Growth yields in bacterial denitrification and nitrate ammonification, *Appl. Environ. Microbiol.*, *73*(5), 1420–1424, doi:10.1128/aem.02508-06.

Teal, J. M., and B. L. Howes (2000), Salt marsh values: Retrospection from the end of the century, in *Concepts and Controversies in Tidal Marsh Ecology*, edited by M. P. Weinstein and D. A. Kreeger, pp. 9–19, Kluwer Acad., Netherlands.

Thamdrup, B., and T. Dalsgaard (2002), Production of N$_2$ through anaerobic ammonium oxidation coupled to nitrate reduction in marine sediments, *Appl. Environ. Microbiol.*, *68*(3), 1312–1318, doi:10.1128/aem.68.3.1312-1318.2002.

Tiedje, J. M., A. J. Sexstone, D. D. Myrold, and J. A. Robinson (1982), Denitrification: Ecological niches, competition and survival, *A. Van. Leeuw. J. Microbiol.*, *48*(6), 569–583.

Uldahl, A. G. (2011), Nitrate reduction processes and plant N status in *Spartina alterniflora* dominated salt marshes, Roskilde University.

Valiela, I. (2015), The Great Sippewissett Salt Marsh plots: Some history, highlights, and contrails from a long-term study, *Estuar. Coast.*, *38*(4), 1099–1120, doi:10.1007/s12237-015-9976-9.

Valiela, I., and J. M. Teal (1979), Nitrogen budget of a salt marsh ecosystem, *Nature*, *280*, 652–656, doi:10.1038/280652a0.

Valiela, I., J. M. Teal, and W. Sass (1973), Nutrient retention in salt marsh plots experimentally fertilized with sewage sludge, *Estuar. Coast Mar. Sci.*, *1*(3), 261–269, doi:10.1016/0302-3524(73)90039-x.

Valiela, I., J. M. Teal, and W. J. Sass (1975), Production and dynamics of salt marsh vegetation and effects of experimental treatment with sewage sludge: Biomass, production and species composition, *J. Appl. Ecol.*, *12*(3), 973–981, doi:10.2307/2402103.

VanZomeren, C. M., J. R. White, and R. D. DeLaune (2012), Fate of nitrate in vegetated brackish coastal marsh, *Soil Sci. Soc. Am. J.*, *76*, 1919–1927, doi:10.2136/sssaj2011.0385.

Vieillard, A. M., and R. W. Fulweiler (2012), Impacts of long-term fertilization on salt marsh tidal creek benthic nutrient and N$_2$ gas fluxes, *Mar. Ecol. Prog. Ser.*, *471*, 11–22, doi:10.3354/meps10013.

White, D. S., and B. L. Howes (1994), Long-term ^{15}N-nitrogen retention in the vegetated sediments of a New England salt marsh, *Limnol. Oceanogr.*, *39*(8), 1878–1892, doi:10.4319/lo.1994.39.8.1878.

Zhang, L., M. A. Altabet, T. X. Wu, and O. Hadas (2007), Sensitive measurement of NH$_4^+$ ^{15}N/^{14}N (δ^{15}NH$_4^+$) at natural abundance levels in fresh and saltwaters, *Anal. Chem.*, *79*(14), 5297–5303, doi:10.1021/ac070106d.